Acta Oceanol. Sin., 2018, Vol. 37, No. 9, P. 59–66
DOI: 10.1007/s13131-018-1264-7
http://www.hyxb.org.cn
E-mail: hyxbe@263.net

Paleoenvironmental implications of the calcium isotope characteristics in the MD81349 from the Nintyeast Ridge in the Indian Ocean

WANG Feng[1], FANG Nianqiao[2*], HU Chaoyong[3], GOLDSMITH Sarah[4], XU Yonghang[1], DING Xuan[2], WANG Aijun[1], CHEN Ping[5], BAO Rui[6]

[1] Third Institute of Oceanography, State Oceanic Administration, Xiamen 361005, China

[2] Institute of Marine Geology and Geophysics, China University of Geosciences (Beijing), Beijing 100083, China

[3] School of Earth Sciences, China University of Geosciences, Wuhan 430074, China

[4] Demo Laboratory, Ctd. MicroMass, Mantchestt M139PL, United Kingdom

[5] School of Earth Science Environmental Engineering, Anhui University of Science and Technology, Huainan 232001, China

[6] Climate and Environment Sciences Laboratory of the institute Pierre Simon Laplace (LSCE), Gif sur Yvette 75000, France

Received 23 October 2017; accepted 23 March 2018

Abstract

A δ^{44}Ca curve from shells of the planktonic foraminifera *Globigerinoides sacculifer* in calcareous biogenic oozes has been extracted from the Nintyeast Ridge in the Indian Ocean since 300 ka. By combining terrigenous inputs (e.g., grain size, magnetic susceptibility, and turbidite frequency) with the oceanic productivity (e.g., biogenic content and *Neogloboquadrina dutertrei* content), it is found that the curve's variations are closely related to the historical evolution of the oceanic calcium cycle. The δ^{44}Ca value is in lower tendency and has small oscillation during Marine Isotope Stage (MIS) 6, when the supply of terrigenous detrital is highest. In contrast, during MIS 3, 5 and 7, the δ^{44}Ca values are in higher tendency, and their fluctuations are consistent with the variations of the productivity proxies. These results suggest that the calcium isotopes are mainly influenced by the input of the Himalayan erosion products to the northern Indian Ocean. In addition, the developmental stages of calcareous planktons may have a secondary impact on the fluctuations of the calcium isotope ratio of sea water.

Key words: Nintyeast Ridge, calcium isotope, paleoceanography, Indian Ocean

Citation: Wang Feng, Fang Nianqiao, Hu Chaoyong, Goldsmith Sarah, Xu Yonghang, Ding Xuan, Wang Aijun, Chen Ping, Bao Rui. 2018. Paleoenvironmental implications of the calcium isotope characteristics in the MD81349 from the Nintyeast Ridge in the Indian Ocean. Acta Oceanologica Sinica, 37(9): 59–66, doi: 10.1007/s13131-018-1264-7

1 Introduction

The variations of light isotope ratios, such as those of oxygen and carbon, have positive correlations with paleoceanographic conditions. In contrast, calcium isotopes of the paleoenvironmental implications are not well constrained (e.g., Russell et al., 1978; Skulan et al., 1997; De La Christina and DePaolo, 2000; Farkaš et al., 2007; Griffith et al., 2008a). Calcium is an important component of the pelagic plankton shells that participate in the cycles of a lithosphere, a hydrosphere and a biosphere, however, the calcium isotopic fractionation characteristics during sedimentation are still limited (Farkaš et al., 2007; Griffith et al., 2008a; Fantle, 2015). The ^{44}Ca to ^{40}Ca fractionation effect due to biological activity and variations in the water temperature during carbonate precipitation has drawn significant attention over the past decade (e.g., Skulan et al., 1997; Zhu and Macdougall, 1998; Nägler et al., 2000; Gussone et al., 2004, 2009; Hippler et al., 2006; Griffith et al., 2008a, b; Kısakürek et al., 2011).

There are six stable isotopes of calcium in nature, ^{40}Ca (96.941%), ^{42}Ca (0.647%), ^{43}Ca (0.135%), ^{44}Ca (2.086%), ^{46}Ca (0.004%) and ^{48}Ca (0.187%). On the basis of the abundances, fractionation characteristics and detection precision of each isotope, the ratio of ^{44}Ca abundance to ^{40}Ca is a widely used proxy for a paleoenvironmental analysis (Heuser et al., 2002; Gussone et al., 2005; Schiller et al., 2012).

Ca^{2+} in the ocean mainly originates from the terrigenous input, the eruption of suboceanic basaltic lava, and hydrothermal activity. Ca^{2+} precipitates from sea water mainly through biological activity and forms calcium carbonate. Imbalances between the input and output of calcium causes variations of the Ca^{2+} concentration in sea water and may also lead to the fluctuations of the ^{44}Ca/^{40}Ca ratio (De La Christina and DePaolo, 2000). Skulan et al. (1997) suggested that the δ^{44}Ca value of basaltic rocks was approximately 0, the δ^{44}Ca value of sea water was approximately 0.90×10^{-3}, and the δ^{44}Ca value of biological calcareous shells was approximately 1.00×10^{-3} lower than that of the surrounding sea water. De La Christina and DePaolo (2000) showed that the δ^{44}Ca values of modern seawater fluctuate between 0.80×10^{-3} and 0.92×10^{-3}. The average δ^{44}Ca value of the hydrothermal fluids

Foundation item: The National Programme on Global Change and Air-sea Interaction under contract Nos GASI-03-04-01-03 and GASI-GEOGE-03; the Research Grant of Third Institute of Oceanography, State Oceanic Administration under contract No. 2015015.
*Corresponding author, E-mail: fangnq@yeah.net

that are associated with mid-ocean ridge basalt (MORB) is -0.61×10^{-3}. Differences in the petrological characteristics and degree of weathering of terrigenous matters lead to large differences in the δ^{44}Ca values in different river basins. For example, the δ^{44}Ca values vary from -0.63×10^{-3} in the Changjiang (Yangtze) River to -1.68×10^{-3} in the Ganges. The δ^{44}Ca values of the calcareous shells of foraminifera and coccolithophores correlate well with that of the surrounding seawater but are generally 1.20×10^{-3}–1.30×10^{-3} lower; the δ^{44}Ca values of corals and Holocene carbonate oozes are even lower, with an average of -2.15×10^{-3}. The δ^{44}Ca values of organic bodies show that the lighter Ca^{2+} are preferentially taken up and fixed in shells, which causes a positive shift of the residual δ^{44}Ca value in the surrounding sea water compared with the initial value. These characteristics can be used to develop a general model of the oceanic calcium cycle and calcium isotope fractionation (Fig. 1).

When carbonate matter precipitates from sea water, the effect of the water temperature has attracted much attention. Skulan et al. (1997) proposed that the δ^{44}Ca values of the foraminifera shells were related to the temperature, but the relationship was very weak. In contrast, De La Christina and DePaolo (2000) proposed that the δ^{44}Ca features of foraminifera shells were not related to the seawater temperature. Zhu and Macdougall (1998) noted that the ^{44}Ca/^{40}Ca values in the shells of shallow-water planktonic foraminifera such as *Globigerinoides sacculifer* and *Neogloboquadrina pachyderma* tended to be heavier during the warm period (Holocene) than during colder periods and in deep water. On the basis of an analysis of the calcium isotopes of cultured living foraminifera and ancient foraminifera shells, Nägler et al. (2000), Sime et al. (2005) and Gussone et al. (2003, 2004) concluded that the δ^{44}Ca values of the calcareous of foraminifera were related to the temperature of the sea water in which they grew due to fractionation. Thus, the temperature effect on the calcium isotopic fractionation that is observed in laboratories cannot be ignored. However, calcium isotopes curve obtained in core is affected by kinds of interferences and bondages, including a variety of factors composite. To make clear which factors dominant the calcium isotopes curve significantly, we need to conduct detailed analyses based on the actual conditions. We selected a single species of foraminifera (*G. sacculifer*) from the northern Indian Ocean and measured its ^{44}Ca/^{40}Ca ratios with a multiple-collector inductively coupled plasma mass spectrometer (MC-ICP-MS). Then we got a δ^{44}Ca curve that spans 300 ka and discussed the characteristics of the calcium isotope variations of the foraminifera shells and their geological implications in paleoenvironment.

2 Materials and methods

The foraminifera shells were collected from a 4.3 m core (MD81349) in the Nintyeast Ridge (01°01′S, 89°22′E, water depth of 2 505 m) (Fig. 2). The foraminifera content in the MD81349 core was significantly higher than that of cores from the nearby ODP758, DSDP216 and DSDP217 stations. The information of sites involved in this study is in Table 1. The oxygen and carbon isotope from the shells of *G. ruber* have been tested at the Climate and Environment Sciences Laboratory of the Institute Pierre Simon Laplace (LSCE) and the National Centre of Scientific Research (CNRS) in France. Biological particles and *N. dutertrei* content data have been finished at the Institute of Marine Geology and Geophysics, China University of Geosciences (Beijing).

In this study, we collected samples from the MD81349 core every 5 cm in the same layers with the oxygen and carbon isotope analysis. A total of 92 samples were collected from the core. Each sample was carefully rinsed and ten *G. sacculifer* individuals with sizes of 315–425 μm were selected, rinsed with deionized water three times, and subjected to ultrasonication for 3 min. We then dissolved them in 8 mL of 5% HNO_3 solution in a teflon bottle and put the solution in the MC-ICP-MS to measure the calcium isotope ratios. The sample analysis was conducted at the Demonstration Laboratory of the MicroMass Company in Manchester, UK. We put 3 mL of the fully dissolved solution in the special sample chamber of the instrument and set up the measurement parameters to count the number of atoms with mass numbers of 39.0, 40.0, 42.0, 43.0, 43.5 and 44.0. The analysis procedure followed the repeating sequence of standard-sample-

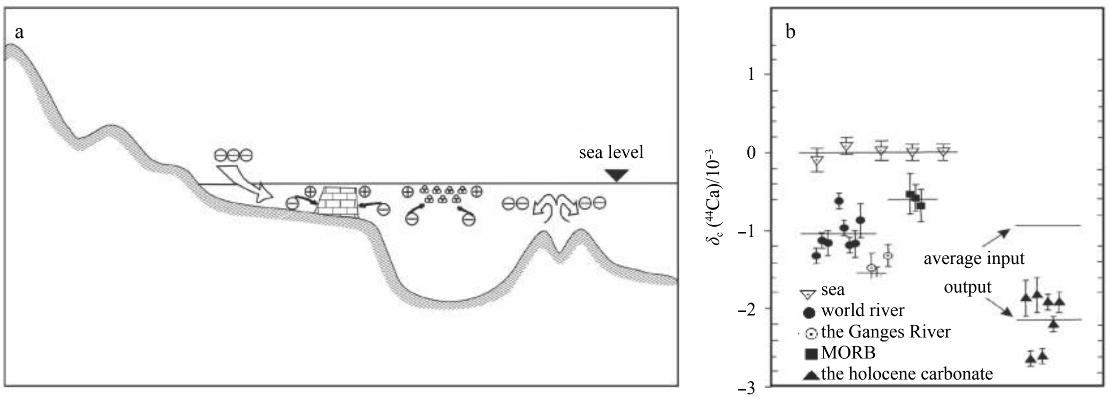

Fig. 1. Circulation model of calcium isotope in the ocean. a. Oceanic calcium isotope distribution model: three circles with minus mean that the input of terrigenous erosion products decreases the most of the calcium isotope ratio; two circles with minus mean ocean floor volcanic eruptions decrease the isotope calcium ratio, but the decrease is smaller than that associated with terrigenous input; and shallow-marine carbonate platforms and pelagic planktonic foraminifera have similar effects on the calcium output; they preferentially take up light isotopes, which increases the background isotope ratios of the regional seawater; one circle with minus means that shallow-marine carbonate platforms and pelagic planktonic foraminifera have similar effects on the calcium output, which absorb the light calcium isotopes from the water into the shell and result in a positive deviation of calcium isotopes in the sea water that expressed by a circle with plus; b. calcium isotope distribution in different river system which is modified according on Zhu and Macdougall (1998).

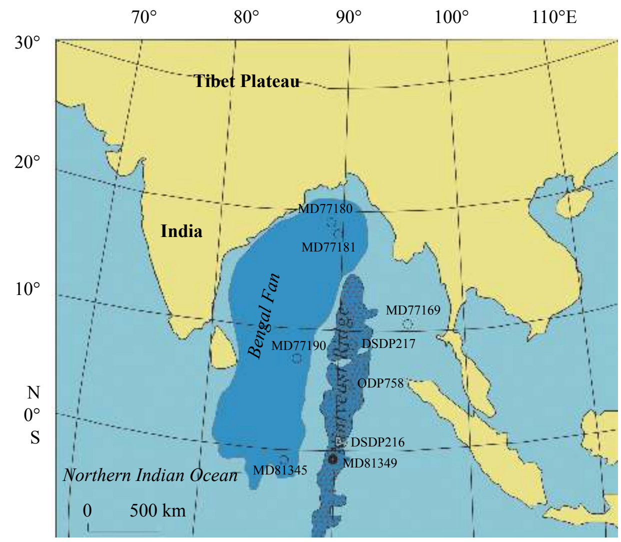

Fig. 2. Location of the study core and their neighbouring geographic circumstances.

standard-sample. The raw data were first corrected for potassium interference to determine the concentration of ^{40}Ca in the solution. The data were then corrected for strontium (Sr^{2+}) Sr^{2+} inferences on the Ca isotopes using the 43.5 signal (corresponding to Sr^{2+}) to determine the concentrations of ^{44}Ca, ^{43}Ca and ^{42}Ca in the same solution. Finally, the data were calibrated using NIST SRM915 a (Standard Reference Materials 915 a, National Institute of Standards and Technology, US Department of Commerce) as the standard reference to obtain the ^{44}Ca and ^{40}Ca data and to yield the curve that represents the variation in δ^{44}Ca since 275 ka. The resolution of δ^{44}Ca measurement is lesser than 0.01%。

3 Results

The ridge sediment was mainly composed of marine biogenic matter. In the past 250 ka, a deposition rate was generally 1.0–2.0 cm/ka (Fang, 1987). On the basis of previous studies (Foucault and Fang, 1987; Ding et al., 1999, 2000, 2003; Fang et al., 2001a, 2002, 2004, 2009), the ridge sediment sequence that is contained in the MD81349 core was continuous and contains many environmental signals that can be used for global comparisons or that reflect significant regional events.

The δ^{18}O curve, which can be used to distinguish eight oxygen isotope stages (Fig. 3), corresponded well to that of the LR04 stack (Lisiecki and Raymo, 2005) . Our δ^{18}O curve was also supported by chronological evidence from the Toba ash layer (75 ka) at a depth of 121–126 cm and the last-appearance datum of pink *G. ruber* (128 ka) in the study area (Ninkovich et al., 1978; Fang, 1990; Paillard et al., 1996).

The main δ^{44}Ca values range from -0.29×10^{-3} to 1.02×10^{-3}. The maximum value of the δ^{44}Ca curve for the *G. sacculifer* shells in the Core MD81394 is 1.52×10^{-3} (in MIS 5.5), and the minimum is -0.99×10^{-3} (in MIS 6.2) (Table 2). The variation curve which takes on low tendency in the glacial periods but high tendency in the interglacial periods does not show fully corresponding to the glacial-interglacial cycles (Fig. 4). In addition, the δ^{13}C curve of the foraminifera shells do not entirely correspond to the glacial/inter-glacial alternations. This phenomenon is due to the oceanic productivity. The values of biological content range from 1 200 to 15 000 g^{-1}. The high value is in the interglacial periods, while the low value in the glacial periods. There is a biological event in 160 ka when the biological particles content value is the lowest. *N. dutertrei* content, as one of the effective productivity proxies, changed mainly same with biological content (Fig. 4).

4 Discussion

In the research of the northern Indian Ocean sedimentary records since 300 ka, the predecessors (Fang et al., 2004, 2009) have pointed out that the MIS 6 is the most significant period which is characterized by the strongest terrigenous input and the remarkable ecological events. In our study, the characteristic of δ^{44}Ca also can be interpreted to the latest evidence for this view.

Generally, the basic characteristics of the δ^{44}Ca curve take on the low tendency in the glacial periods, the high tendency in the interglacial periods, but peak value is not consistent with an oxygen isotope change curve, which is focused on discussing in our study (Fig. 4).

There are two different kinds of sedimentary types in the northern Indian Ocean: Bengal Fan sedimentary type and Nintyeast Ridge sedimentary type. The former is mainly Himalayan erosion which carried by turbidity; the latter is pelagic sediments which is the calcareous ooze. Although their compositions and sedimentary types are great difference, their sedimentary processes are influenced all together by the regional tectonic uplift, the sea level change and chemical properties of sea (Fang et al., 2009). Thus, the sedimentary processes can refer to each other. In our study, the core we research is from the Nintyeast Ridge, which does not suffer the turbidity activity directly. In order to explore the control factors of δ^{44}Ca, we widely cited the predecessors' results in the Bengal fan as a reference, such as magnetic susceptibility, grain size, turbidite layers (proxy), which can reflect terrigenous input change.

Although the overall pattern of low values in the glacial periods and high values in the interglacial periods prior to MIS 4.0 is similar to the oscillation of the δ^{18}O curve and represents climatic cycles. What interests us is that, the peak positions of the two

Table 1. The location information of the cores

	Length/m	Latitude	Longitude	Water depth/m	Data source
MD81349	4.30	01°01′S	89°22′E	2 505	this study
MD81345	5.40	01°09′S	87°45′E	4 372	Fang et al. (2004)
MD77180	13.70	19°12′N	88°30′E	1 986	Fang et al. (2004)
MD77181	13.96	17°23′N	90°27′E	2 271	Fang (1987)
MD77190	12.00	07°41′N	87°49′E	3 740	Fang (1987)
MD77169	14.60	10°12′N	95°03′E	2 360	Fang et al. (2004)
ODP758	676.80	5°23′N	90°22′E	2 924	Fang et al. (2004)
DSDP216	477.50	1°28′N	90°12′E	2 247	Fang et al. (2004)
DSDP217	614.50	8°56′N	90°32′E	3 020	Fang et al. (2004)

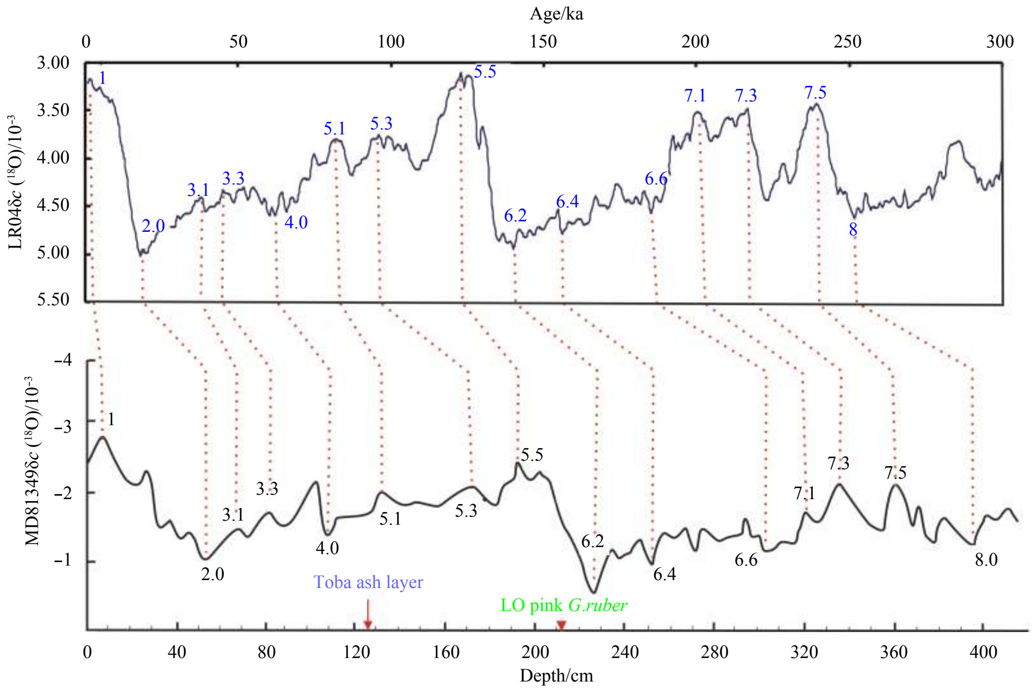

Fig. 3. The chronology for Site MD81349 for the upper 300 ka. The LR04 δ^{18}O stack and its age mode provide the paleoclimate community with an important stratigraphic tool, which be used to facilitate the comparison of widely distributed marine climate records (Lisiecki and Raymo, 2005).

Table 2. δ^{44}Ca of Core MD81349

Depth/cm	$\delta c(^{44}Ca)/10^{-3}$	Depth/cm	$\delta c(^{44}Ca)/10^{-3}$	Depth/cm	$\delta c(^{44}Ca)/10^{-3}$	Depth/cm	$\delta c(^{44}Ca)/10^{-3}$
1	0.17	106	0.05	221	0.18	319	0.95
6	0.20	111	0.12	226	0.07	324	0.39
11	0.33	116	0.17	231	0.09	329	0.34
16	0.22	118	0.03	234	0.07	334	0.40
21	0.34	127	0.27	236	−0.01	336	0.25
26	0.19	131	0.26	241	0.04	339	0.03
31	0.26	136	0.29	246	0.28	344	−0.01
36	0.00	141	0.47	251	0.12	349	0.09
41	−0.29	146	0.27	256	0.02	354	−0.07
46	0.25	151	0.27	261	0.04	359	0.48
51	0.74	156	0.33	266	0.18	364	0.17
56	0.28	161	−0.20	271	−0.03	367	0.35
61	0.32	171	0.48	276	0.18	369	0.22
66	0.24	176	0.44	281	0.11	374	1.02
71	0.77	181	1.52	291	0.38	377	0.48
76	0.42	186	0.14	293	0.26	379	0.24
81	0.29	189	0.21	296	0.18	384	0.17
86	0.33	191	0.59	299	0.20	389	0.34
91	0.02	196	0.31	302	0.34	394	0.25
96	0.18	201	0.29	304	0.33	399	0.09
98	−0.15	206	−0.99	309	0.20	404	0.23
101	0.36	211	0.09	312	0.23	409	0.36
103	0.62	216	0.01	315	0.24	413	0.32

curves differ greatly. It indicates that the δ^{44}Ca values in the foraminifera shells are not closely related to cold and warm conditions during MIS 5.5, which is characterized as a typical warm climate in the δ^{18}O curve. For example, the relationship between the δ^{44}Ca curve and the glacial/interglacial alternations since MIS 4.0 is unclear. MIS 5.5 generally follows the low-value characteristics of MIS 6.0, and MIS 5.4 and 5.3 contain the maximum peak value of the entire record. From MIS 5.3 to the early part of MIS 3.0, the curve is relatively flat but has some rhythmic characteristics. During MIS 3.0 and 2.0, the trend of the δ^{44}Ca curve is generally opposite to that of the δ^{18}O curve; however, during the Holocene, the δ^{18}O curve contains a negative peak value because

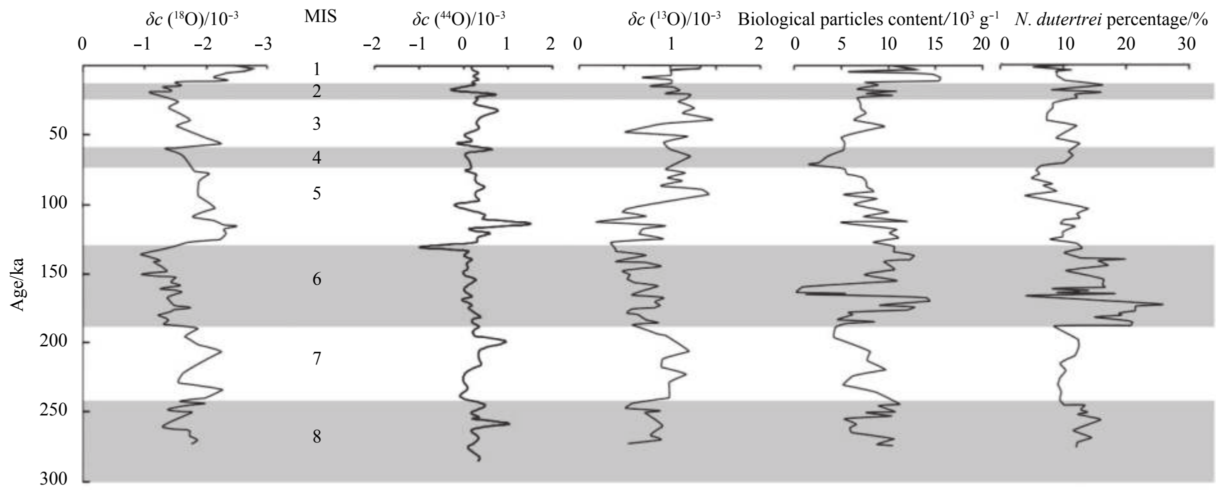

Fig. 4. The variation curves of δ^{44}Ca compared to the other environmental proxies since MIS8 in the core of Site MD81349.

of the global glacial retreat, but the δ^{44}Ca curve remains at intermediate levels. It is well known that the δ^{18}O curve is a signal corresponding to the variations of SST and global ice sheet, characterized by oscillating between the glacial periods and the interglacial periods. With reference to Fig. 4, we can see that the oscillation characteristic of our δ^{44}Ca curve can vary with the δ^{18}O one neither on the whole nor in detail. As a result, we argue that the SST may bring little influence to the pattern of δ^{44}Ca curve.

There are several explanations for this observation. (1) Although the experimental results of Nägler et al. (2000) indicate that δ^{44}Ca varies due to the water temperature, their study only shows reactions under simple laboratory conditions that are not representative of the synergistic environmental effects under complex natural conditions. If their conclusion that every 1°C change in temperature is equivalent to a variation of (0.24±0.02) $\delta c(^{44}Ca)$ is directly applied to estimating the surface sea temperature of the Indian Ocean over the past 200 ka, the maximum temperature difference could be 6.0–11.0°C, which is not realistic and thus is hard to accept. (2) The δ^{44}Ca curve does not display any significant peaks during warm periods such as the Holocene and MIS 5.5. In contrast, the δ^{44}Ca curve contains an interval with prominent high values around the last glacial maximum. (3) During several transition zones of the glacial/interglacial periods, such as the MIS 8.0, 7.0 and 4.0 transitions, the peak δ^{44}Ca values cannot be explained by increasing the surface sea temperature.

As is showed by the overall fluctuations of the δ^{44}Ca curve in the MD81349 core, the primary controlling factor should be related to the operation of the oceanic calcium cycle system. Skulan et al. (1997) and Zhu and Macdougall (1998) specifically addressed the issue of the calcium cycle. Owing to the different standards that they used, they obtained different δ^{44}Ca values for the background sea water, ocean ridge basalt, hydrothermal fluids, ancient carbonate rocks, aluminosilicate minerals, river discharges and modern organism skeletons (shells) (Fig. 1). However, they shared several common characteristics. The δ^{44}Ca values were highest in the sea water, and the δ^{44}Ca values of the ocean-floor volcanic eruption products were lower than that of sea water but higher than those of other calcium-rich materials. In addition, the δ^{44}Ca values were lowest in carbonate rocks (sediment), which were mainly controlled by biological sedimentation. In addition, the data of Skulan et al. (1997) show that the input of terrigenous erosion products from river systems to the ocean can generate very low δ^{44}Ca values. De La Christina and DePaolo (2000) showed that the disequilibrium between terrigenous erosion products and biogenic sedimentation could cause a significant drift in the Ca^{2+} isotope composition of sea water. The variations in the ratio between the terrigenous Ca input flux due to weathering and the Ca output flux of biogenic sedimentation in the ocean over the past 80 Ma that they obtained showed a significant reverse evolutionary relationship to the marine carbonate δ^{44}Ca record(De La Christina and DePaolo, 2000). The δ^{44}Ca values in rocks were approximately -0.44×10^{-3} and reached 0 during the late Eocene (ca. 40 Ma). However, from the Oligocene to the mid-Miocene (ca. 34–15 Ma), the input of light calcium components far exceeded the precipitation of light calcium components by the skeletons and shells of calcareous marine organisms due to the significant increase in the weathering and denudation of terrigenous carbonate rocks and the enhanced input of calcium-bearing erosion products to the oceans. Therefore, the δ^{44}Ca record contains a low-value interval that lasts for nearly 20 Ma. Hodell and Woodruff (1994) note that the $^{87}Sr/^{86}Sr$ ratio in the sea water contain a period of rapid increases between 20 and 16 Ma, which indicate that terrigenous erosion and discharge from the Himalaya and the Tibetan Plateau significantly impact the oceanic chemical components.

The ^{44}Ca curve characteristics of high values in the (sub-) interglacial periods and low values in the (sub-) glacial periods during MIS 5.0–8.0 (Fig. 4) may also be related to the variations in the terrigenous input flux to the northern Indian Ocean. The ^{44}Ca value in carbonate materials are lower than that provided by silicates. Himalayan erosion products is carried to the whole Ganges delta(Fang, 1990, 2001a). Owing to the uplift of the Tibetan Plateau and the large exposure of carbonate rocks in the Greater Himalaya, the terrigenous input of the Ganges was characterized by extremely low ^{44}Ca values. The sedimentary record of the Bengal deep-sea fan shows that the amount of terrigenous input is controlled by glacial sea-level variations (Foucault and Fang, 1987; Fang, 1990). This suggests that enhanced rock weathering during (sub-) glacial periods, especially the large amounts of erosion products that are carried across the continental shelf to pelagic regions, would inevitably decrease the δ^{44}Ca value of the sea water. In contrast, as the sea level rises during (sub-) interglacial periods, the terrigenous input fluxes to the oceans decrease, and thus, the ^{44}Ca in the seawater is likely to remain high.

Note that all of the sedimentary records in the northern Indian Ocean show that the intensity of the terrigenous input during MIS 6.0 was the highest of the past 300 ka (Fig. 5). Fang et al. (2001a) pointed out that the terrigenous input is carried by the turbidity current to the south of 10°S in the Indian Ocean Basin, which reflects the turbidite activity influences widely in our study area. Turbidite activity is dominated by terrigenous input activities. When the turbidite layers appear, it means the terrigenous input to the ocean. Although the turbidite layer does not appear in the Core MD81349 directly, the sedimentary process of Core MD81349 is also affected by the terrigenous input. Through the turbidite layer records in the other cores of the Bengal Fan which can illustrate the terrigenous input to the Bengal Fan (Fig. 5), we can see that the Cores MD77181, MD77190 and MD81345 have the turbidite layers in MIS6.0. The grain size and the calcium carbonate content show that the terrigenous input has a strong influence on our study area in MIS 6.0 and a biological event happened in 160 ka (Fang et al., 2001a; Zhang, 2002). The significant ecological events between 169 and 160 ka led to a severe oceanic productivity crisis in the study area (Fang et al., 2001b, 2004). The anomalously high input and low output of Ca led to an interval of low δ^{44}Ca values during MIS 6.0 (Figs 4 and 5). As we know, the terrigenous input means a plenty of compound of iron, such as magnetite are carried into the sediment, magnetic susceptibility corresponding appears high value. Figure 5 shows that when the magnetic susceptibility of MD77181, MD77180 and MD77169 is high value in MIS 6.0, the δ^{44}Ca takes on the low tendency, which demonstrates the terrigenous input makes the δ^{44}Ca value low. Meanwhile, the turbidite activity of the MD77181, MD77190 and MD81345 intensively in MIS 6.0 which are dominated by the terrigenous transport activities also prove that the amount of the terrigenous input in MIS 6.0 lead to the low δ^{44}Ca in our study area. The transport of terrigenous carbonate weathering products to the ocean mainly occurs through real ionic solutions and rarely leaves a visible sedimentary record in the oceans as silicate; therefore, the ^{44}Ca/^{40}Ca ratio in calcareous shells could be an effective monitoring proxy for the terrigenous carbonate input.

The factors that affect the δ^{44}Ca curve after MIS 5.0 are more complicated. The glacial sea-level cycles continue to affect the terrigenous input and ultimately control the δ^{44}Ca variations in the foraminifera shells. However, the developmental stages of biogenic sediments affected the final results (i.e., the feedback of the new distribution of δ^{44}Ca in the sea water to the shell record). In fact, during MIS 6.0 and 7.0, the productivity underwent significant fluctuations (Fang et al., 2004). However, due to the large differences in the terrigenous input fluxes, the δ^{44}Ca characteristics of the foraminifera shells are not consistent. For example, during MIS 7.1 (ca. 200 ka), the sedimentary records in the northern Indian Ocean generally show increasing trends of oceanic productivity, of which the main characteristics include more abundant planktonic foraminifera and radiolarians, higher *N. dutertrei* contents in the plankton foraminifera, and increased Gd/Ca ratios in the calcareous shells. During this period, because of the low terrigenous input, the effect of the high productivity produced peak zones in the δ^{44}Ca that were recorded by organism shells. Nonetheless, due to the increase in the terrigenous input during MIS 6.0 and despite the significantly higher productivity than in MIS 7.0 during certain periods, the discharge of ^{40}Ca-rich continental erosion products in the study area generally masked the fluctuations that were due to the productivity. The δ^{44}Ca record from the MD81349 core shows that except for special periods like MIS 6.0, most of the calcium isotope oscillation patterns correspond well to variations in productivity. The characteristics of the variations in the substitute proxies, such as the sedimentary flux of the foraminifera as well as δ^{13}C and *N. dutertrei*, indicate that they significantly affect the formation of the δ^{44}Ca peaks. The Bengal deep-sea fan and the adjacent areas are the centre of terrigenous accumulation in the northern Indian Ocean. According to more than 30 cores from this area, despite the high sedimentary flux during the last glacial maximum, the sedimentary record of fine grains without any coarse sand indicates that the intensity of the terrigenous input is less than that during the other glacial periods that are represented by MIS 4.0 and 6.0. Thus, the productivity effect was clearly reflected in the δ^{44}Ca record. Records of high productivity during MIS 5.0 are rare

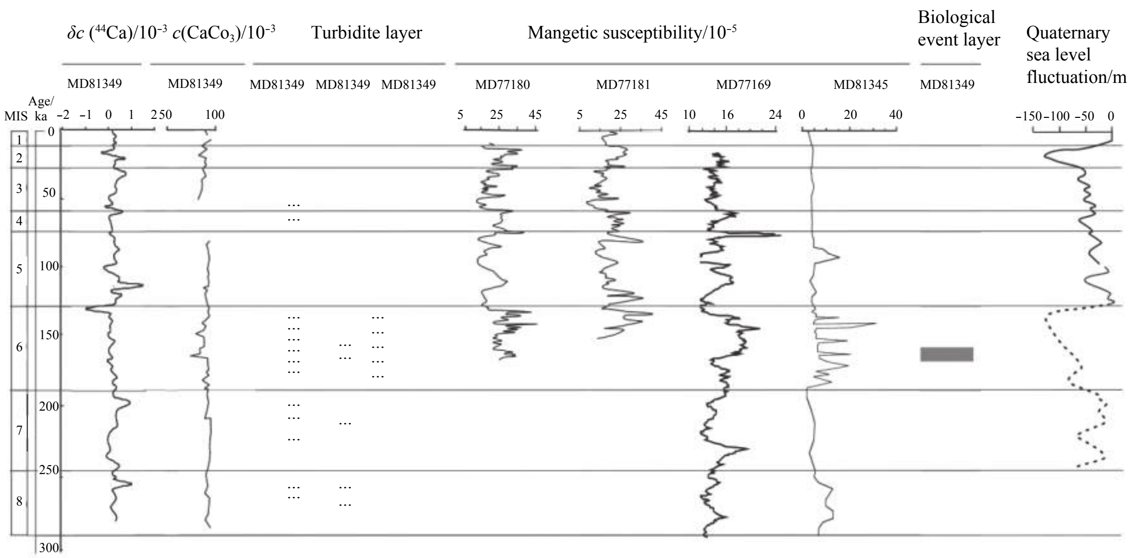

Fig. 5. The proxies of MD81349 compared with other different cores' in the study area (MD77180, MD77181 refer to Li et al. (2006); MD77190 refer to Fang et al. (1999); MD77169 refer to Fang et al. (2001a); MD81345 refer to Fang et al. (2001a); Quaternary sea level fluctuations refer to Chappell and Shacklenton (1986)).

in the northern Indian Ocean. However, because of rising sea level, the terrigenous input reached the minimum of the 300 ka sedimentary history (Foucault and Fang, 1987), which led to the maximum peak of δ^{44}Ca in that period. However, the maximum interval of δ^{44}Ca does not occur during stage MIS 5.5, when the sea level was the highest and the terrigenous input was the lowest; rather, it lags by more than 10 ka.

We propose two explanations for this. (1) The low δ^{44}Ca values in the seawater due to the strong terrigenous input during MIS 6.0 remained significant during the early part of MIS 5.0. (2) The ubiquitous strong dissolution effect of calcareous shells during the early part of MIS 5.0 in the study area allowed more ^{40}Ca to participate in the sediment-sea water-sediment cycles. The only problem with these explanations is that according to the biogenic fractionation effect, the evolutions of the δ^{44}Ca and δ^{13}C curves should be relatively consistent in terms of reflecting oceanic productivity. However, in MD81349, the δ^{44}Ca variation from 115 to 100 ka is exactly opposite to the δ^{13}C trend. Considering the biological data from this core, δ^{44}Ca reflects the productivity fluctuations during MIS 2.0 to 5.0 even more strongly than δ^{13}C. In other words, the ubiquitous increases in the δ^{13}C values in the northern Indian Ocean at approximately 100 ka do not necessarily indicate significant increases in regional productivity.

5 Conclusions

(1) The Ca cycle (i.e., the input and output of oceanic calcium) can directly affect the light and heavy Ca isotopic compositions of sea water. This characteristic is easy to observe at high resolution despite the long residence time of calcium in sea water. The fluctuations of δ^{44}Ca in *G. sacculifer* shells from the MD81349 station at the Nintyeast Ridge are useful for investigating environmental changes over the past 300 ka in the study area.

(2) In the Ca cycle system, the terrigenous input to the ocean is likely to be the key factor that controls the δ^{44}Ca curve. The sedimentary record due to the terrigenous input from the erosion of carbonate rocks in the Himalaya clearly reflects this factor. The terrigenous input to the northeastern Indian Ocean over the past 300 ka is most prominent during MIS 6.0. The characteristics of the δ^{44}Ca variations in the study area provide additional evidence from a new perspective.

(3) Oceanic productivity is also related to the calcium output, which is an important factor for δ^{44}Ca variation in addition to the terrigenous input. While changes in the seawater temperature theoretically and experimentally affect Ca isotopic fractionation, they do not significantly impact the δ^{44}Ca curve due to the synergistic effects of important environmental factors, such as terrigenous input and oceanic productivity output.

Acknowledgements

The authors are grateful to the laboratory staff, the ship's crew and the students for making the hard effort to this article. Many thanks to Demo Laboratory, Ctd. MicroMass, for testing δ^{44}Ca.

References

Chappell J, Shacklenton N J. 1986. Oxygen isotopes and sea level. Nature, 324(6093): 137–140

De La Christina L, DePaolo D J. 2000. Isotopic evidence for variations in the marine calcium cycle over the Cenozoic. Science, 289(5482): 1176–1178

Ding Xuan, Fang Nianqiao, Chen Xuefang. 1999. Planktonic foraminifera during late quaternary in the Bengal Bay and their paleoceanographic implications. Geoscience (in Chinese), 13(1): 37–42

Ding Xuan, Fang Nianqiao, Chen Ping, et al. 2003. Upwelling actions in the bay of Bengal during marine isotope stages 2 and 3: evidence for Indian winter monsoon. Quaternary Sciences (in Chinese), 23(1): 53–59

Ding Xuan, Fang Nianqiao, Wan Xiaoqiao. 2000. Monsoon climate and its paleoceanographic records of the bay of Bengal during Late Quaternary. Geoscience (in Chinese), 14(3): 295–300

Fang Nianqiao. 1987. Le controle climatique de la sedimentarion Quatemative Recente Dans La region moyenne Du come Profond du gange (Ocean Indian) [dissertation]. Paris: Paris University Pierre et Marie Curie

Fang Nianqiao. 1990. Climatic and glacio-eustatic control over the recent quaternary sedimentation in the northeast Ganges deep sea fan. Geoscience (in Chinese), 4(1): 10–22

Fang Nianqiao, Chen Xuefang, Ding Xuan, et al. 2001b. Paleoceanographical records under impact of the Indian monsoon from the Bengal Deep Sea Fan and Ninetyeast Ridge during the last 260 ka. Science in China Series D: Earth Sciences, 44(1): 351–359

Fang Nianqiao, Chen Xuefang, Hu Chaoyong, et al. 2001a. Deep sea sedimentary records in the northeastern Indian ocean and their response to the uplift of the Qinghai-Xizang Plateau. Quaternary Sciences (in Chinese), 21(6): 490–499

Fang Nianqiao, Ding Xuan, Chen Xuefang, et al. 1999. Rapid climatic change in oxygen isotope stage 3: evidence from the rhythmic sedimentary record in core MD77190, Bengal Bay. Quaternary Sciences (in Chinese), 19(6): 511–517

Fang Nianqiao, Ding Xuan, Liu Yongqin, et al. 2002. Pelagic sedimentary records of the Ninetyeast Ridge and the late Cenozoic important tectono-environmental events. Earth Science Frontiers (in Chinese), 9(1): 103–111

Fang Nianqiao, Ding Xuan, Hu Chaoyong, et al. 2004. A significant paleoceanographic event taking place in northeastern Indian ocean during oxygen isotope stage 6. Earth Science—Journal of China University of Geosciences (in Chinese), 29(3): 127–134

Fang Nianqiao, Ding Xuan, Zhang Zhenguo, et al. 2009. Two types of deep-water sedimentary sequence in northeastern Indian Ocean and their response to the Himalayan Uplifts. Scientia Geologica Sinica (in Chinese), 44(4): 1181–1198

Fantle M S. 2015. Calcium isotopic evidence for rapid recrystallization of bulk marine carbonates and implications for geochemical proxies. Geochimica et Cosmochimica Acta, 148: 378–401

Farkaš J, Böhm F, Wallmann K, et al. 2007. Calcium isotope record of Phanerozoic oceans: Implications for chemical evolution of seawater and its causative mechanisms. Geochimica et Cosmochimica Acta, 71(21): 5117–5134

Foucault A, Fang Nianqiao. 1987. Climatic control of the quaternary sedimentation in the bay of Bengal. Comptes Rendus de l' Academie des Sciences Serie IIa: Sciences de la Terre et des Planets, 305(17): 1383–1388

Griffith E M, Paytan A, Kozdon R, et al. 2008a. Influences on the fractionation of calcium isotopes in planktonic foraminifera. Earth and Planetary Science Letters, 268(1–2): 124–136

Griffith E M, Paytan A, Bullen T D. 2008b. Evidence for a dynamic marine calcium cycle during the past 30 million years from a record of calcium isotopes in marine barite. Geochimica et Cosmochimica Acta Supplement, 72(12): A329

Gussone N, Eisenhauer A, Heuser A, et al. 2003. Model for kinetic effects on calcium isotope fractionation (δ^{44}Ca) in inorganic aragonite and cultured planktonic foraminifera. Geochimica et Cosmochimica Acta, 67(7): 1375–1382

Gussone N, Eisenhauer A, Tiedemann R, et al. 2004. Reconstruction of caribbean sea surface temperature and salinity fluctuations in response to the Pliocene closure of the Central American Gateway and radiative forcing, using $\delta^{44/40}$ Ca, δ^{18}O and Mg/Ca ratios. Earth and Planetary Science Letters, 227(3–4): 201–214

Gussone N, Böhm F, Eisenhauer A, et al. 2005. Calcium isotope fractionation in calcite and aragonite. Geochimica et Cosmochimica Acta, 69(18): 4485–4494

Gussone N, Hönisch B, Heuser A, et al. 2009. A critical evaluation of calcium isotope ratios in tests of planktonic foraminifers.

Geochimica et Cosmochimica Acta, 73(24): 7241–7255

Heuser A, Eisenhauer A, Gussone N, et al. 2002. Measurement of calcium isotopes (δ^{44}Ca) using a multicollector TIMS technique. International Journal of Mass Spectrometry, 220(3): 385–397

Hippler D, Eisenhauer A, Nägler T F. 2006. Tropical Atlantic SST history inferred from Ca isotope thermometry over the last 140ka. Geochimica et Cosmochimica Acta, 70(1): 90–100

Hodell D A, Woodruff F. 1994. Variations in the strontium isotopic ratio of seawater during the Miocene: stratigraphic and geochemical implications. Paleoceanography, 9(3): 405–426

Kısakürek B, Eisenhauer A, Böhm F, et al. 2011. Controls on calcium isotope fractionation in cultured planktic foraminifera, *Globigerinoides ruber* and *Globigerinella siphonifera*. Geochimica et Cosmochimica Acta, 75(2): 427–443

Li Haiyan, Zhang Shihong, Fang Nianqiao, et al. 2006. Magnetic records of Core MD77-181 in the Bay of Bengal and their paleoenvironmental implications. Chinese Science Bulletin, 51(15): 1884–1893

Lisiecki L E, Raymo M E. 2005. A Pliocene - Pleistocene stack of 57 globally distributed benthic δ^{18}O records. Paleoceanography and Paleoclimatology, 20(1): PA1003

Nägler T F, Eisenhauer A, Müller A, et al. 2000. The δ^{44}Ca–temperature calibration on fossil and cultured *Globigerinoides sacculifer*: new tool for reconstruction of past sea surface temperatures. Geochemistry, Geophysics, Geosystems, 1(9): 2000GC000091

Ninkovich D, Shackleton N J, Abdel-Monem A A, et al. 1978. K-Ar age of the late Pleistocene eruption of Toba, north Sumatra. Nature, 276(5688): 574–577

Paillard D, Labeyrie L, Yiou P. 1996. Macintosh program performs time-series analysis. Eos, Transactions American Geophysical Union, 77(39): 379–379

Russell W A, Papanastassiou D A, Tombrello T A. 1978. Ca isotope fractionation on the earth and other solar systerm materials. Geochimica et Cosmochimica Acta, 42(8): 1075–1090

Schiller M, Paton C, Bizzarro M. 2012. Calcium isotope measurement by combined HR-MC-ICPMS and TIMS. Journal of Analytical Atomic Spectrometry, 27(1): 38–49

Sime N G, De La Rocha C L, Galy A. 2005. Negligible temperature dependence of calcium isotope fractionation in 12 species of planktonic foraminifera. Earth and Planetary Science Letters, 232(1–2): 51–66

Skulan J, DePaolo D J, Owens T L. 1997. Biological control of calcium isotopic abundances in the global calcium cycle. Geochimica et Cosmochimica Acta, 61(12): 2505–2510

Zhang Zhenfang. 2002. Sedimentary records and paleoclimate evolution of Bay of Bengal since Pliocene time [dissertation]. Beijing: China University of Geosciences

Zhu Peng, Macdougall J D. 1998. Calcium isotopes in the marine environment and the oceanic calcium cycle. Geochimica et Cosmochimica Acta, 62(10): 1691–1698